A NEW NUCLEAR BUT NON RADIOACTIVE METHOD FOR RAPID ELEMENTAL ANALYSIS OF CLAYS

G. Demortier, G. Hoffelt-Fontaine

L.A.R.N., Facultés Universitaires de Namur, 22, rue Muzet, B-5000 Namur, Belgium

Abstract—A method using the bombardment of samples with protons and other positive ions of energy in the MeV range is described: the prompt atomic (X-rays) and nuclear (γ-rays and charged particles) events generated during the bombardment, are detected with energy sensitive solid state detectors: cooled Ge(Li) for γ-rays and hard X-rays, cooled Si(Li) detectors for soft X-rays (3–20 keV) and Si-barrier detectors for charged particles. These 3 types of detectors can be simultaneously used for multipurpose experiments. These techniques are particularly useful for simultaneous detection of all the elements of interest in the sample. Comparisons are made with other microtechniques. Analyses of Li, Na, K, Ca, Rb, Cs and Cl exchanged in appropriate chloride solutions have been achieved for several clays (Geisenheim, Isola di Ponza, Layton). A new phenomenon relative to the anion contribution in cation exchangers is observed. A method of profile analysis of Na by resonant nuclear reactions is discussed.

INTRODUCTION

During the past twenty years, nuclear physicists have developed numerous techniques, often sophisticated, for the study of atomic nuclei. The first part of this important development was specially devoted to achieving high stability and energy resolution of the low energy (up to 5 MeV) accelerators, the most used accelerator being the Van de Graaff machine. The second part took place in the field of high resolution γ-ray, X-ray and charged particle spectroscopy, and was made possible through the improvement in the performance of the cooled solid state detectors. It is now possible to analyse, at the same time, characteristic X-rays and γ-rays of nearly all the elements of the periodic table. The accuracy of determination of the energy of these photons ranges between 1% for 1 keV X-ray to 1.5‰ for 2 MeV γ-rays.

The use of low energy particle accelerators for excitation of nuclei and the utilization of solid state detectors for identification of the nuclei offer great promise for development of research in other sciences, particularly in chemical analysis (Deconninck *et al.*, 1972a).

Unfortunately, the purposes of fundamental research in nuclear physics are not the same as those of applied physics and for this reason, few extensive and accurate data exist for nuclear reaction induced by charged particles. However, at present, several physicists are looking at the particular subject of charged particles inducing nuclear reaction and some laboratories like ours (L.A.R.N.) have been equipped for research such as chemical analysis. Although L.A.R.N. was created by physicists, the subject of the studies dealt with is mostly furnished by other scientists such as chemists, biologists, geologists, mineralogists, dentists, physicians and others.

The aim of this paper is to present the basic physical principles of quantitative elemental analysis using prompt atomic and nuclear reactions and to discuss their applications to clays and minerals. More details on the technique may be found in literature as quoted in reference to previous papers of our group (mainly G. Deconninck and G. Demortier).

1. EXPERIMENTAL ARRANGEMENT

The typical arrangement of the laboratory is shown in Fig. 1. The accelerated particles (mainly protons and alpha particles) are focused, through evacuated pipes, to different target sites, using electromagnetic deflection. Passing through adjustable slits, the energy of the incident particle can be determined to 1 keV for 1 MeV protons. The vacuum in the whole machine is 10^{-5} Torr.

The samples to be analysed being also in the vacuum, must be solids with low vapor pressure, but it is also possible to make analysis at atmospheric pressure as discussed by Deconninck (1973a). The electronic pulses from energy dispersive solid state detectors proportional to the energy of the photon (or charged particle) are analysed by a sophisticated electronic system, the final stage being the storage and the treatment of information in a small (8 k) computer.
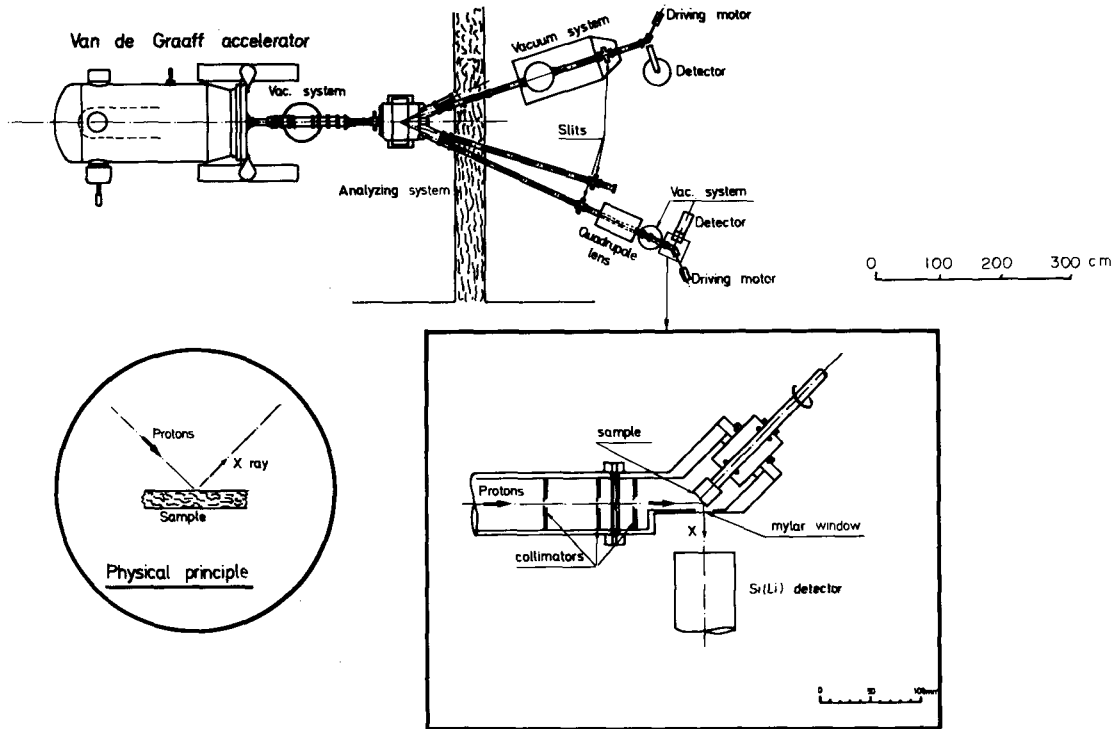
2. PHYSICAL PRINCIPLES OF ANALYSIS

When low energy protons interact with nuclei, three types of (useful) reactions may be produced. These are:

nuclear reactions with emission of charged particles (2.1).

Coulomb excitation and resonance reactions giving rise to γ-emission (2.2).

atomic interaction with electrons of inner shells followed by X-ray emission (2.3).

ELEMENTAL ANALYSIS BY γ and X RAYS DETECTION

Fig. 1. Typical experimental arrangement for elemental analysis by proton bombardment and X-ray detection.

Each of these types of reaction are induced in a very short time (10^{-9} to 10^{-20} sec) and may be called prompt reactions by comparison with delayed emission of radiations in neutron activation analysis.

2.1. α-particle emission.

The first type of reaction, emission of charged particles, is of great interest for the purpose of analysis of very low mass elements.

Table 1(a). Energies E_α (in MeV) of the α particles emitted in the backward direction by low mass elements bombarded with protons of different energies

Element	E_p = 700 keV	E_p = 1 MeV	E_p = 2 MeV
^6Li	1.36	1.34	1.35
^7Li	7.74	7.65	7.48
^8Be	1.26	1.32	1.57
^{10}B	0.85	0.93	1.25
^{11}B	5.48	5.52	5.75
	3.68	3.73	4.02
^{12}C	0	0	0
^{13}C	0	0	0
^{14}N	0	0	0
^{15}N	3.81	3.91	4.35
	0.73	0.85	1.35
^{16}O	0	0	0
^{17}O	1.25	1.38	1.93
^{18}O	3.36	3.48	4.01
^{19}F	6.61	6.72	7.23
	1.97	2.10	2.68

Table 1(b). Energies E_α (in MeV) of the α particles emitted in the backward direction by low mass elements bombarded with deuterons of different energies

Element	E_d = 700 keV	E_d = 1 MeV	E_d = 2 MeV
^6Li	9.49	9.28	8.72
^7Li	6.72	6.59	6.31
^9Be	4.02	4.00	4.02
^{10}B	10.90	10.82	10.68
	9.08	9.02	8.94
	3.85	3.85	3.95
^{11}B	5.10	5.10	5.22
	3.99	4.01	4.16
	3.56	3.58	3.75
	3.18	3.21	3.39
^{12}C	0	0	0
^{13}C	3.61	3.66	3.93
	2.18	2.25	2.56
	0.70	0.78	1.15
^{14}N	9.68	9.69	9.85
	6.53	6.56	6.79
	4.27	4.32	4.61
	2.90	2.96	3.28
^{15}N	5.67	5.72	6.01
	3.46	3.53	3.88
	3.04	3.12	3.47
	2.93	3.00	3.36
^{16}O	2.48	2.57	2.98
	0.87	0.97	1.42
^{17}O	7.54	7.59	7.91
	3.60	3.69	4.09
	3.58	3.66	4.07
	2.81	2.91	3.33
	2.21	2.31	2.75
^{18}O	3.47	3.57	4.00
	3.38	3.48	3.91
	3.25	3.35	3.78
	3.17	3.27	3.71
^{19}F	7.99	8.06	8.43
	7.31	7.39	7.78
	5.62	5.70	6.12
	5.02	5.11	5.53

Table 1 gives the energies of the characteristic α-particles emitted during the bombardment by protons and deuterons of different energies, by low mass elements. For a particular energy of the incident protons, the energy of the α-particles emitted in the backward direction with respect to the proton trajectory is a characteristic of the bombarded elements.

The determination of the energy of the α-particles allows a rapid identification of the elements present in the sample. By counting the pulses in a peak, it is possible to make a quantitative analysis of this particular element. The choice of the energy of the incident protons is very important to avoid interferences between several elements. For example it is possible to separate α-particles from Li and F at $E_p = 1$ MeV but not at $E_p = 2$ MeV (see Table 1a).

For a time of bombardment of 10 min. with a proton beam of 10 nA, the detection sensitivity is about 200 ppm for Li, 50 ppm for B, 2000 ppm for F, and several % for O and N. For a longer time of bombardment (about one hour) and an intensity of the proton beam of 1 μA, the sensitivity for boron may reach 10 ppb in a sample containing less than 400 ppm of N. For Li the maximum sensitivity may reach 1 ppm (Demortier, 1974a; Ligeon and Bontemps, 1972).

By increasing the energy of the incident protons, it is possible to induce nuclear reactions in deeper slices of a thick target material. As the energy of the protons increases, the quantity of the analysed sample increases, but the counting rate of the emitted particles does not always increase in the same ratio so that the sensitivity of the technique is not necessarily increased. When the nuclear reactions are induced in deeper slices, the outgoing particles must lose some of their energy in coming out of the samples and consequently the peaks are broadened and interference between elements often occurs as for Li and F with 2 MeV protons. For Li and B the best energy range is between 400 to 700 keV.

For traces of some other elements such as nitrogen, (d,α) reactions induced by the bombardment with deuterons of 2 MeV allow one to achieve a sensitivity of 50 ppm (Debras, 1975).

2.2. γ-ray emission

The first type of reactions (the emission of charged particle induced by low energy protons) may be generated only on very light nuclei. The coulombic repulsion between the incident positive ion and the positive atomic nucleus does not allow the proton to penetrate in heavy nuclei, and even when the incident particle penetrated, the resulting alpha particle cannot escape from the target. Fortunately, when the emission of charged particles is forbidden, the quantum mechanical behavior of nuclear interactions allows other types of reactions, such as γ-ray emission. This kind of reaction has been known for a long time: resonance capture and inelastic scattering for medium weight nuclei, coulombic interaction for heavy nuclei.

The case of medium weight nuclei from F to Cl is particularly interesting. Let us take the case of aluminum. When a thick target of pure Al is bombarded with protons of increasing energy, the intensity of the γ-rays increases, step by step (Fig. 2). Just under 1 MeV, the intensity of the γ-rays is 450 per μC of incident protons and per unit solid angle of detection. By increasing the proton energy by a small amount the intensity increases suddenly by a factor of 2. This means that when protons have just an energy of 992 keV, they have a great probability to form a compound nucleus of excited ^{28}Si:

$$^{27}\text{Al} + p = {}^{28}\text{Si}^* \rightarrow {}^{28}\text{Si} + \gamma(E_\gamma = 1.778 \text{ MeV}).$$
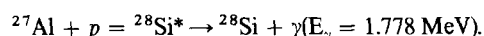
This compound nucleus is formed in a well-defined energy state and returns to its fundamental state by emission of characteristic γ-rays. For protons of 992 keV, the great majority of the emitted 1778 keV γ rays comes from the surface of the sample. If we now slowly increase the energy of the protons, the intensity of these γ rays stays at a constant level. As the incident proton progressively loses its energy in the Al target, this particular energy of 992 keV is reached several tenths of a micron deeper under the surface, but the first tenths of a micron does not give rise to γ emission, because no level of ^{28}Si exist for those incident proton energies.

For protons of 992 keV, γ-rays comes from the surface (Fig. 3) and from several deeper slices of the sample corresponding to less intense resonances at lower proton energies. For a slightly higher energy of the protons, say 1 MeV, these γ-rays come from other (deeper) slices of the sample. For homogeneous materials, this particular shape of the intensity of γ-rays with increasing energy of the protons is of no importance. But for inhomogeneous samples, we have here a method to measure profiles of concentration. Suppose that we have only Al nuclei in a deep slice
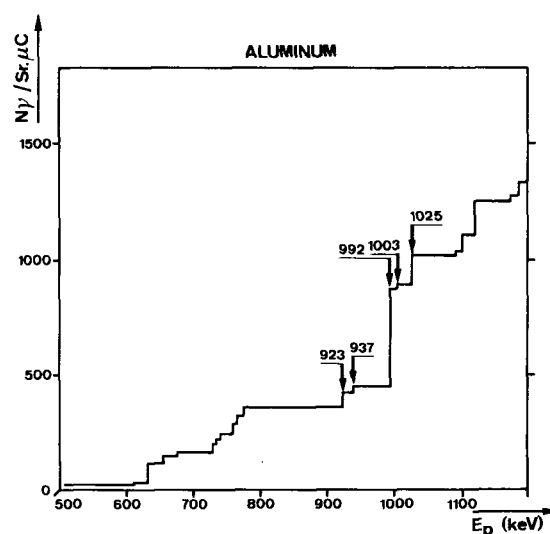

Fig. 2. Stepwise variation of the intensity of the 1778 keV γ-rays produced during the bombardment of pure Al with protons of increasing energy.
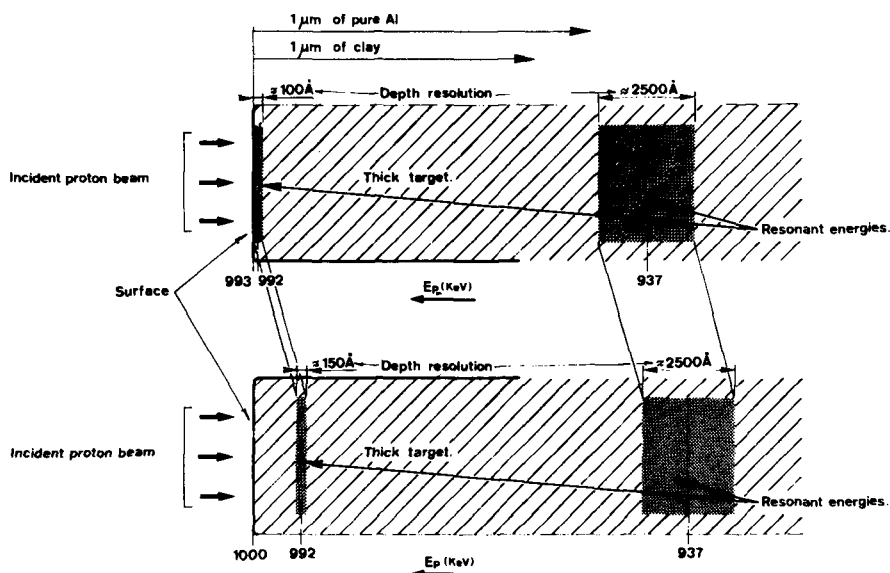
Fig. 3. Regions of the sample where 1778 keV γ-rays from Al are produced for 993 and 1000 keV incident protons.

of the sample, the intensity of γ-rays will only be non zero if a resonant energy is achieved just in the slice.

Comparing the intensity curve obtained by the bombardment of the sample of interest with that obtained by the bombardment of a pure Al sample, it is possible to obtain (perhaps after sophisticated calculations and a long time of measurement) the concentration profile of Al. The depth resolution of this technique (due to the statistical behavior of the energy loss in the sample) lies between 100 and 200 Å near the surface and 2500 Å at a few microns below the surface for an incident proton beam with 1 keV energy resolution. Taking into account the high number of resonances and the energy straggling of the incident particles slowing down in the material the determination of the concentration profile is only possible if high variation of Al concentration occurs in the first five μm under the surface of the bombarded sample.

This special shape (step by step) of the intensity curve of the γ emission vs the energy of the protons has been studied at L.A.R.N. on F, Na, Mg, Al, P, S and Cl. For heavier nuclei the intensity curves rise only smoothly (as it may be seen in Fig. 4 for four characteristic γ-rays of Ag). No compound nucleus may be formed with those nuclei because of the coulombic repulsion; only excitation of the nucleus by electromagnetic interaction is possible (Deconninck et al., 1972b; Demortier et al., 1972a and 1975b).

The sensitivity of the (p,γ) technique for elements is given in Table 2. The ranges given here depend on the background of radiation in the region of the characteristic peak (Deconninck and Demortier, 1972b; Demortier et al., 1975a).

Let us look now at the interference and absorption problems. The interaction of γ-rays with matter is very different from the interaction of charged particles with matter. The γ-ray energies are always constant

while their number may vary with the thickness of the material to be crossed. For (p,γ) reactions, in which the energy of γ rays lies between 100 keV and several MeV, this attenuation of the number of γ rays in thickness reached by the decelerated protons (about 10 μm) is of no importance. Interference between element is a more stringent restriction, as it may be seen in Table 2: the same γ-ray may be
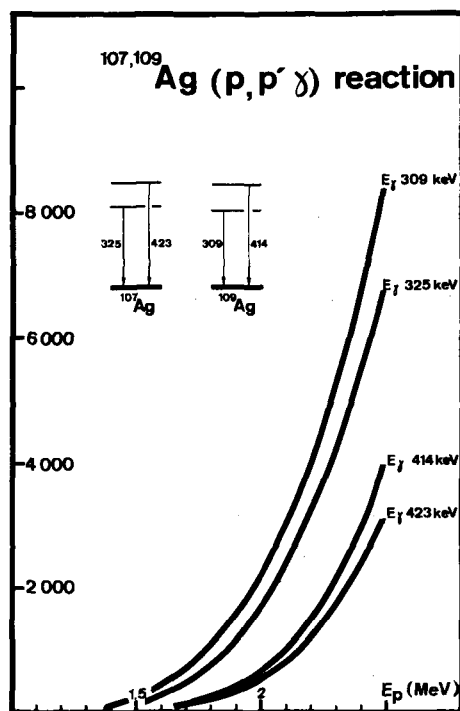

Fig. 4. Smooth variation of the intensity of 309, 325, 414 and 423 keV γ-rays produced during the bombardment of pure silver with protons of increasing energy.

Table 2. Energies of the γ-rays emitted by elements during the bombardment with 2.5 MeV protons. Best measured sensitivity. Possible interfering elements

Element	Eγ (keV)	Origin of γ rays	Sensitivity	Possibility of interference
Li	477	$^{7}Li(p,p'\gamma)^{7}Li$	500 ppm	
C	2357	$^{12}C(p,\gamma)^{13}N$	1%	
F	110	$^{19}F(p,p'\gamma)^{19}F$		O (W)
	197	$^{19}F(p,p'\gamma)^{19}F$	100 ppb	O
Na	439	$^{23}Na(p,p'\gamma)^{23}Na$	5 ppm	
	1368	$^{23}Na(p,\gamma)^{24}Mg$		Mg,Al
	1630	$^{23}Na(p,\alpha\gamma)^{20}Ne$		
Mg	170	$^{26}Mg(p,\gamma)^{27}Al$		Al
	390	$^{25}Mg(p,p'\gamma)^{25}Mg$		
	586	$^{25}Mg(p,p'\gamma)^{25}Mg$	100 ppm	
	843	$^{26}Mg(p,\gamma)^{27}Al$		Al (S)
	976	$^{25}Mg(p,p'\gamma)^{25}Mg$		
	1013	$^{26}Mg(p,\gamma)^{27}Al$		Al
	1368	$^{24}Mg(p,p'\gamma)^{24}Mg$		Na,Al
Al	170	$^{27}Al(p,p'\gamma)^{27}Al$		Mg
	843	$^{27}Al(p,p'\gamma)^{27}Al$	100 ppm	Mg (S)
	1013	$^{27}Al(p,p'\gamma)^{27}Al$	50 ppm	Mg
	1368	$^{27}Al(p,\alpha\gamma)^{24}Mg$		Na,Mg
	1778	$^{27}Al(p,\gamma)^{28}Si$		Si,P
Si	1273	$^{29}Si(p,p'\gamma)^{29}Si$	0.5%	
	1778	$^{28}Si(p,p'\gamma)^{28}Si$		Al,P
P	1266	$^{31}P(p,p'\gamma)^{31}P$	500 ppm	S
	1778	$^{31}P(p,\alpha\gamma)^{28}Si$		Al,Si
	2237	$^{31}P(p,\gamma)^{32}S$		S,Cl
S	806	$^{32}S(p,\gamma)^{33}Cl$		
	842	$^{33}S(p,p'\gamma)^{33}S$		(Mg),(Al)
	1220	$^{34}S(p,\gamma)^{35}Cl$		Cl
	1266	$^{34}S(p,\alpha\gamma)^{31}P$		P
	1763	$^{34}S(p,\gamma)^{35}Cl$		Cl
	2237	$^{32}S(p,p'\gamma)^{32}S$	1%	P,Cl
Cl	1220	$^{35}Cl(p,p'\gamma)^{35}Cl$	1%	S
	2127	$^{37}Cl(p,\alpha\gamma)^{34}S$		
	2168	$^{37}Cl(p,\gamma)^{38}Ar$		
	2237	$^{35}Cl(p,\alpha\gamma)^{32}S$		P,S
V	320	$^{51}V(p,p'\gamma)^{51}V$	1%	
Cr	126	$^{54}Cr(p,\gamma)^{55}Mn$		Mn,Fe
	379	$^{52}Cr(p,\gamma)^{53}Mn$	500 ppm	
	783	$^{50}Cr(p,p'\gamma)^{50}Cr$		
	913	$^{52}Cr(p,\gamma)^{53}Mn$		
	1292	$^{52}Cr(p,\gamma)^{53}Mn$		
Mn	126	$^{55}Mn(p,p'\gamma)^{55}Mn$	100 ppm	Cr,Fe
	413	$^{55}Mn(p,n\gamma)^{55}Fe$	0.1%	Ag
	595	$^{55}Mn(p,p'\gamma)^{55}Mn$		
	847	$^{55}Mn(p,\gamma)^{56}Fe$		Fe
	933	$^{55}Mn(p,n\gamma)^{55}Fe$	200 ppm	
	1035	$^{55}Mn(p,\gamma)^{56}Fe$		

emitted under the bombardment of more than one element with protons. For example 1778 keV γ-ray may be emitted during the bombardment of Al, Si or P with protons and all the γ-rays characteristic of P may interfere with those from other nuclei.

Fortunately, solving this kind of interference is often easy, as explained in Table 3 for the particular case of P. If all the γ rays of an element are observed, the ratio of the height of the full energy peaks of these γ-rays can be checked accurately and this ratio is a characteristic of the bombarded element. In cases of low concentration for which only the most intense peak is observable (like the 1266 keV for P) it is possible to check the presence of S which also emits 1266 keV γ-rays together with 842 and 2237 keV γ-rays but with an intensity considerably higher than that of 1266 keV γ-ray. The comparison of the ratios of the intensities of the two peaks (842 and 2237 keV lines) with that obtained for pure S, may solve the interference and it becomes possible to attribute to S and P their own intensity (Demortier and Bodart, 1972a). If the sensitivity for medium weight elements is good for (p,γ) reactions, it is bad for heavier elements for which it is not better than 1%.

2.3. X-ray emission

The third phenomenon (X-ray production under proton bombardment) will give an answer to this limitation. The proton losing its energy in the thick sample, removes electrons from their specific shells. When a hole is created in the K shell, rearrangements occur with emission of K X-rays (and Auger electrons specially for low mass elements). For the medium weight elements, it is possible to observe two X-ray lines (K_α and K_β) with a good Si(Li) detector; for heavier elements, 4 lines ($K_{\alpha 1}$, $K_{\alpha 2}$, $K_{\beta 1}$ and $K_{\beta 2}$) may be detected. The ratios of the intensities of these lines are known and do not vary very much with the chemical environments of the elements (Tamaki, 1975). In the following we will designate this technique of charged particle inducing X-rays by CPXR.

The resolution of the energy dispersive detector (cooled Si–Li) used for X-ray detection is 170 eV for 6 keV X-rays and 250 eV for 20 keV X-rays. This resolution is not as good as that obtained for 2θ goniometers but the Si–Li detectors offer 3 advantages over diffraction systems: (1) a bigger solid angle, (2) the possibility of simultaneous detection of numerous different X-ray lines and (3) the possibility of analysis of heavy elements by detection of K X-rays which are less absorbed in the samples than L and M

Table 3. Solution of interferences with phosphorus. The relative intensities of the γ-rays (I_γ) emitted under the bombardment of the same amount of Al, Si, S and Cl with 2.5 MeV protons

Bombarded element		Possible interfering γ-rays		Other emitted γ-rays			
Al	E_γ (keV)	1778		843	1013	1368	
	I_γ	120		2535	5010	670	
Si	E_γ (keV)	1266	1778	1273			
	I_γ	10	160	2350			
S	E_γ (keV)	1266	2237	806	842	1220	1762
	I_γ	8	10	120	755	65	60
Cl	E_γ (keV)	2237		1220	2127	2168	
	I_γ	5		1125	380	900	

X-rays. The probability of production of X-rays by the bombardment of protons is 10^3 to 10^5 times greater than that for γ-rays for proton energies less than 3 MeV (Gordon et al., 1972). This probability increases smoothly with increasing proton energy.

Unfortunately the energies of these X-rays are much lower than those of the γ-rays and corrections for the absorption in the analysed sample may become important. For analysis of thick targets, the ratio of the X-ray yields from the sample and the standard is given by (Demortier, 1974b).

$$\frac{I_{sp}}{I_{st}} = \frac{C_{sp} \int_{E_P}^0 \sigma_x(E) \dfrac{dE}{S_{sp}(E)} e^{-\mu \cdot x_{sp}}}{C_{st} \int_{E_P}^0 \sigma_x(E) \dfrac{dE}{S_{st}(E)} e^{-\bar{\mu} \cdot \bar{x}_{st}}} \qquad (1)$$

where I is the detected X-ray yield, C the concentration of the element of interest, $\sigma_x(E)$ the cross section for the production of the characteristic X-ray of the element for protons of energy E, $S(E)$ the stopping power of the target for incident protons, and

$$\bar{\mu} \cdot \bar{x} = \sum_j \mu_{ij} \int_{E_P}^E \frac{\cos \theta_i}{\cos \theta_0} \cdot \frac{n_j A_j}{\sum n_j A_j S_j(E)} \, dE \qquad (2)$$

the attenuation factor for the X-rays of interest in the target itself, μ_{ij} being the mass absorption coefficient of the particular X-ray of element i by element j, θ_i and θ_0 the angles of the incoming proton trajectory and of the outgoing X-ray with respect to the normal of the polished surface of the target. Subscripts sp and st refer to the sample and the standard respectively. The quantity to be measured C_{sp} is included in $S_{sp}(E)$ and $\bar{\mu}\bar{x}$ and therefore equation (1) is only useful for determination of low quantities of elements in known matrices.

Typical results of calculations of the attenuation factors will be found in Table 4, where we give the percentages of transmitted K_α X-rays of Cl, K, Ca, Rb and L_α X-rays of Cs produced during the bombardment of clays (Geisenheim, Isola di Ponza and Layton) with several energies of the incident protons and for $\theta_0 = \theta_i = 45°$. The choice of the appropriate incident proton energy for rapid quantitative analysis will be discussed later in the section on applications. Physical data on mass absorption coefficients and stopping powers of materials are taken from Williamson

Table 4. Percentages of the transmitted yield of K_α (Cl, K, Ca, Rb) and L_α (Cs) X-rays produced by the bombardment of clays by different proton energies

	E_P (MeV)	Cl	K	Ca	Cs	Rb
GEISENHEIM	0.4	85.3	92.0	93.8	95.3	99.8
	0.7	69.6	82.8	86.4	89.9	99.5
	1.0	54.0	71.8	77.3	83.4	99.1
	1.3	41.0	60.6	67.4	75.7	98.6
	1.7	28.3	47.2	54.8	65.1	97.8
ISOLA DI PONZA	0.4	86.4	92.7	94.5	95.9	99.8
	0.7	71.4	84.0	87.7	90.9	99.6
	1.0	56.2	73.5	79.4	84.8	99.3
	1.3	43.2	62.6	70.0	77.7	99.0
	1.7	30.1	49.3	57.9	67.6	98.3
LAYTON	0.4	86.8	92.9	94.7	96.1	99.8
	0.7	72.0	84.4	88.0	91.4	99.6
	1.0	56.9	74.1	79.8	85.7	99.4
	1.3	43.9	63.3	70.6	79.0	99.0
	1.7	30.7	50.1	58.5	69.2	98.4

Table 5. Computed X-ray yield from each micron under the surface of thick samples of clay (density = 2)

Depth under surface (µm)	$E_P = 700$ keV						$E_P = 1.7$ MeV	
	Cl		K		Ca		Rb	
	X-ray per µm %	X-ray total %	X-ray per µm %	X-ray total %	X-ray per µm %	X-ray total %	X-ray per µm %	X-ray total %
1	28	28	28.5	28.5	29	29	6.5	6.5
2	23	51	23	51.5	22.5	51.5	6.3	12.8
3	18	69	17	68.5	17	68.5	6.2	19
4	13	82	13	81.5	12.5	81	6.0	25
5	8.6	90.6	8.5	90	8.6	89.6	5.9	30.9
6	5.2	95.8	5.3	95.3	5.5	95.1	5.5	36.4
7	2.7	98.5	3	98.3	3.2	98.3	5.4	41.8
8	1.2	99.7	1.3	99.6	1.3	99.6	5.1	46.9
9	0.28	99.98	0.37	99.97	0.37	99.97	4.8	51.7
10	0.02	100	0.03	100	0.03	100	4.6	56.3
11							4.5	60.8
12							4.3	65.1
13							4.0	69.1
14							3.9	73.0
15							3.7	76.7
16							3.2	79.9
17							2.8	82.7
18							2.5	85.2
19							2.2	87.4
20							2.0	89.4
21							1.7	91.1
22							1.5	92.6
23							1.3	93.6
24							1.2	95.1
25							1.0	96.1
26							0.9	97.0
27							0.7	97.7
28							0.6	98.3
29							0.5	98.8
30							0.4	99.2
31							0.3	99.5
32							0.2	99.7
33							0.1	99.8

et al. (1966) and Liebafsky et al. (1960). Results of these calculations are given with an accuracy of 3% in all cases.

For complex samples for which the major elements are not perfectly known, the internal standard technique is often necessary. In this case and for low concentration of the added internal standard, say $q \ll 1$, in the powdered sample under analysis, equation (1) becomes:

$$\frac{I_{sp}}{I_{st}} = \frac{C_{sp}}{C_{sp}(1-q) + q} \qquad (3)$$

the other terms of (1) being nearly the same for the sample and the internal standard (Demortier, 1974b).

The cross sections for production of X-rays by protons being several orders of magnitude higher than for classical X-ray fluorescence, enhancement effects are not important in the CPXR method.

The amount of material needed for a complete analysis is very small. The practical limit comes from the handling of the sample. We give in Table 5 the percentage of the total X-ray yield for each μm of the thick sample of clay: bombarded with 700 keV protons, 90% of the total yield comes from the first 5 μm of the bombarded sample and from the first 20 μm for 1.7 MeV protons. With a proton beam 1 mm dia. commonly used in our laboratory, the useful part of the analysed sample may be less than 10 μg. For a sensitivity of 1 ppm, the lowest amount of detected element is about 10^{-11} g (Deconninck, 1972c; Demortier, 1974c).

3. APPLICATIONS TO MINERALOGY

3.1. Iron determination in gels

Measurements of iron concentration in silica gels and xerogels have been made at L.A.R.N. (in order to study the paramagnetic properties of these substances (Prof. J. J. Fripiat (U.C.L.) Louvain and C.N.R.S. (Orléans)). As the samples are insulators, a thin coating of C was sputtered on the front face in order to avoid accumulation of the positive incident

charges and the resulting bremsstrahlung spectrum generated by the delayed high voltage discharge (low capacity of the target may indeed produce high potential). The samples supported on a good conducting rotating holder do not show apparent destruction during the bombardment with a beam of 5 nA of 1 MeV protons for about 1 min. This short time is sufficient for quantitative determination of 50 ppm of Fe. The spectrum of X-rays detected with Si–Li detector and reproduced in Fig. 5, shows 52 ± 5 ppm of Fe, 43 ± 4 ppm of Cu and traces <10 ppm of Zr. X-ray lines of lower mass elements are suppressed by a small polythene absorber inserted between the target and the detector. Our results are in good agreement with those of Fripiat (1973).

For materials supporting a longer time of bombardment (30 min) the sensitivity of the CPXR technique reaches 1 ppm for elements in the region from V to Zn, 10 ppm for other elements in interference-free analyses. Determination of these low concentrations has been done on fragile biological samples by this technique (Demortier, 1974c).

3.2. Cation exchanges in clays

Bentonites were treated with 0.01, 0.1 and 1.0 molar aqueous solutions of LiCl, NaCl, KCl, RbCl and CsCl. The samples were then repeatedly washed in fixed volumes of distilled water in the laboratory of Professor F. Freund, "Mineralogisch–Petrographisches Institut der Universität zu Köln" (Germany). The amount of Li was determined by the proton induced α emission and γ emission (see 2.1 and 2.2), the amount of Na by proton induced γ emission and the amounts of Cl, K, Ca, Rb and Cs by the CPXR method. It may be observed in Table 4 that for the

analysis of Cl, K, Ca by detection of K_α X-rays and of Cs by detection of L_α X-rays, the incident proton energy is to be chosen as low as possible in order to avoid important absorption in the samples. In order to obtain a sufficient emission rate we have worked with 700 keV protons. For the analysis of Rb an energy of 1700 keV was necessary to improve the sensitivity.

Samples were small disks, 5 mm in dia. and 0.3 mm thick, obtained by pressing the material powder (10 to 20 tons). The conductivity of these samples was sufficient to avoid other handling such as coating as mentioned above. The homogeneity of the material have been determined by small displacements of the target samples in the proton beam.

Typical spectra of γ and X-rays are given in Figs. 6 and 7. Data are reproduced in Table 6. After smoothing of the spectra, the accuracy of determination is better than 10%. For these clays treated in several solutions of cations (0.1 molar) corresponding to one or five times of washing, the amount of Cl retained decreases as one goes from Li to Cs. These results, already observed in cation exchange studies on algae (Demortier et al., 1972b and 1972c), are interpreted by Freund et al. (1975a) who assume a strong interaction between the small cation (Li^+ and Na^+) and the Cl^- anions leading to the formation of associated ion pairs or more complex clusters in the adsorbed state, indicating the Cl^- anions may not be directly bonded to the silicate surface but rather bridged to it via adsorbed cations. This cation–anion interaction is lower with increasing cation radii (K^+, Rb^+, Cs^+). The behavior was less strongly observed for molecular sieve-type zeolites.

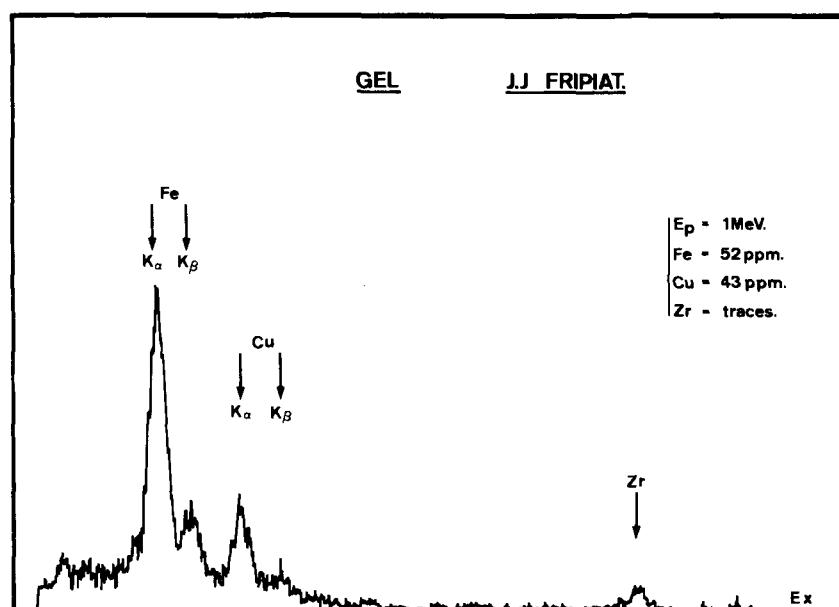The contribution to the covalent bond between Cl and small cations in concentrated solutions of alkali

Fig. 5. X-ray spectrum obtained during the bombardment of gel with 1.5 MeV incident protons.
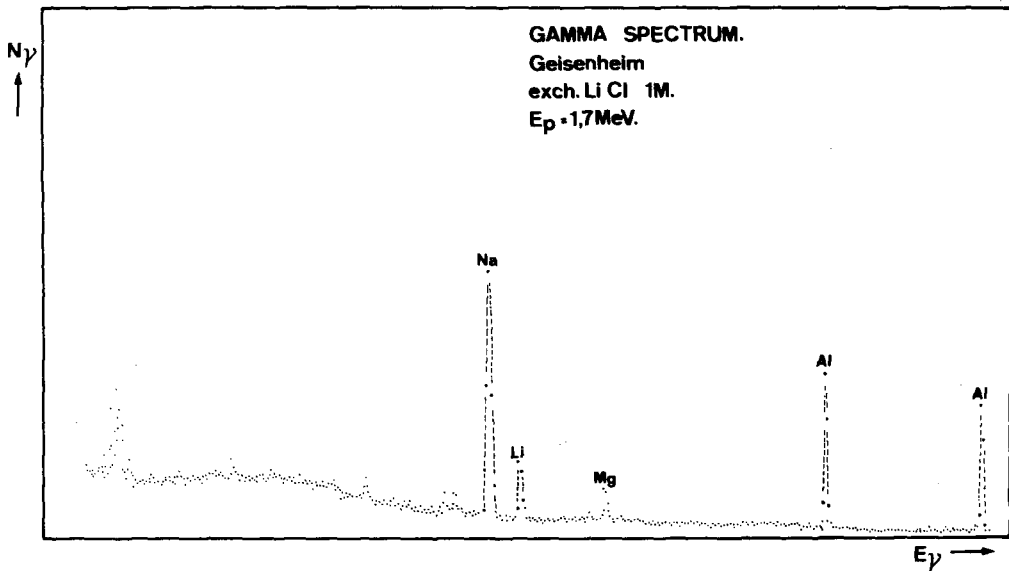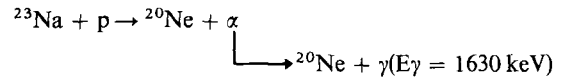
Fig. 6. γ-ray spectrum obtained during the bombardment of Geisenheim clay exchanged in LiCl aqueous solution with 1.7 MeV protons.

chloride was also observed by X-ray spectroscopy of the K_β band of Cl (Freund et al., 1975b).

3.3. Surface analysis of Na in albite

Albite crystals were treated by Professor Jasmund et al. from the "Mineralogisch–Petrographisches Institut der Universität zu Köln" (Germany) in HCl

Fig. 7. X-ray spectra obtained during the bombardment with 700 keV protons of Geisenheim clay exchanged with NH_4OH followed by exchange in CsCl aqueous solution (a) with NaCl aqueous solution (b). Observe the difference in the intensities of the $Cl(K_\alpha)$ peaks.

solutions at 60° for several days in order to test the expected disappearance of Na at the surface of the sample. The polished surface of the crystal was bombarded with protons of increasing energy. The reaction:

$$^{23}Na + p \rightarrow ^{20}Ne + \alpha$$
$$\hookrightarrow ^{20}Ne + \gamma(E\gamma = 1630\,keV)$$

presents the same step by step variations as for Al (see part 2.2 and Fig. 3). During the bombardment with protons of increasing energy from the first resonant (also threshold) energy situated at 1012 keV, nuclear resonant reaction leading to the emission of 1630 keV γ-rays takes place in different slices of the sample under the bombarded surface, allowing concentration profile measurements of Na. The results are shown in Fig. 8. Curve 1 (bottom) refers to the variation of the γ-ray emission with increasing proton energy on an untreated albite sample (dots) and coincides with the same curve obtained during the bombardment of a mixture of NaCl + C of same concen-
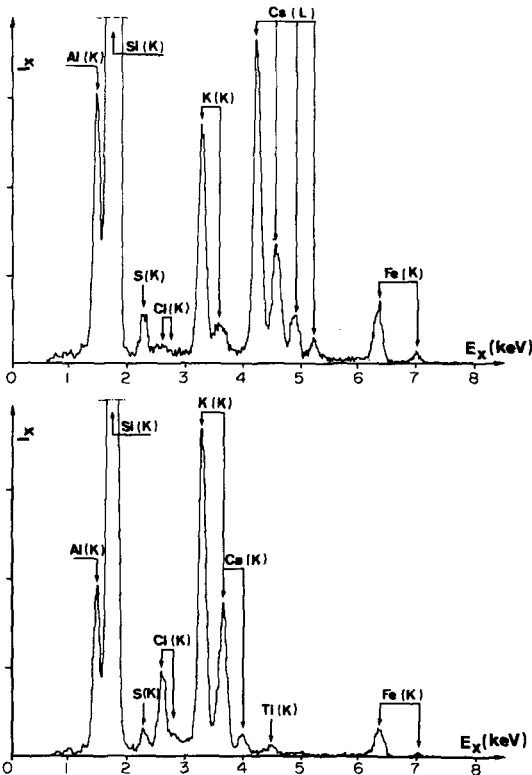
Table 6. Elemental analysis of Geisenheim treated in different solutions of chlorides. Evidence of Cl retention

Observed concentration in %					
clay treated in 0.1 molar chloride solutions washing procedure: one time					
Solution	Li	Na	K	Rb	Cs	Cl
Li Cl	0.26	0.19	0.34	–	–	0.59
Na Cl	0.04	1.50	0.39	–	–	0.44
K Cl	0.05	0.18	0.91	–	–	0.15
Rb Cl	0.05	0.20	0.34	1.46	–	0.11
Cs Cl	0.04	0.19	0.32	–	2.07	0.11
clay treated in 1 molar chloride solutions washing procedure: five times					
Li Cl	0.50	0.12	0.29	–	–	0.20
Na Cl	0.05	1.59	0.40	–	–	0.11
K Cl	0.04	0.13	1.06	–	–	0.02
Rb Cl	0.05	0.14	0.43	1.96	–	0.006
Cs Cl	0.04	0.18	0.35	–	2.26	0.01

tration in Na as the "normal" albite (O). Curve 2 (□) depicts the same results for an albite sample treated for 20 days in HCl solution (pH = 1). It shows partial disappearing of Na in the first 0.6 μm under the surface of the crystal. The top part of the figure indicates the calculated concentration of Na in these 0.6 μm. Sodium profiles are easily measurable by this technique up to 1.5 μm in such mineral samples, with a spatial resolution of 0.05 μm. For deeper slices the method can be applied but with a little more complicated calculation arising from the competition of other resonances at higher energies of the incident protons. The complete measurement is to be made in a short time (1 hour maximum) to avoid migration of diffusible Na by heating of the sample under the proton bombardment. Curve 3 shows the "observed" concentration of Na after 2 hours of bombardment. The increasing concentration of Na in the first 0.1 μm arises after a long time of bombardment but this increase partially disappears after a short time of cooling at room temperature and atmospheric pressure.

Special care has been taken to avoid accumulation of charges at the surface of the sample. Static positive charges produce a positive potential on nonconducting targets and thus cause a shift of the measured resonant energy (to higher energy). As the concentration profile is determined by this shift of the
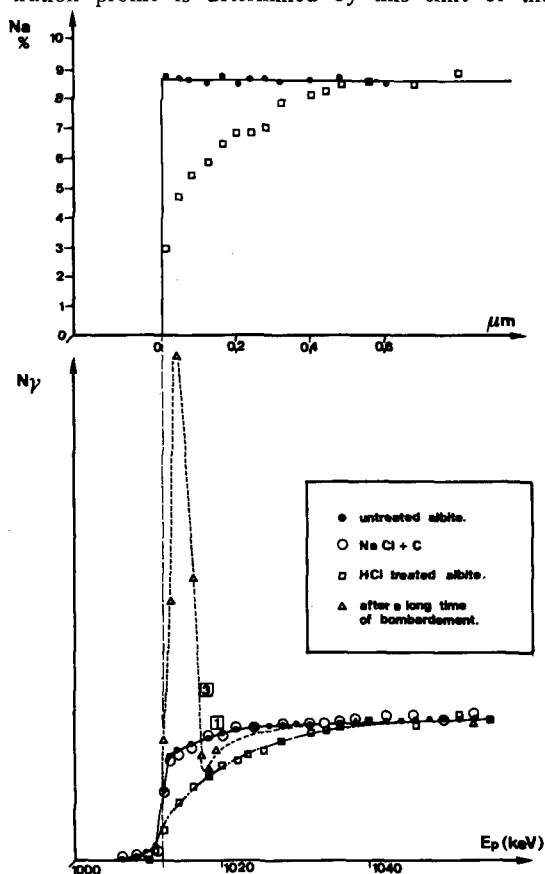

Fig. 8. Depth profile analysis of Na in albite treated in HCl aqueous solution: (a) calculated concentration of Na, using the comparison (b) of the intensities of the γ-rays from the resonant nuclear reaction $^{23}Na(p,\alpha\gamma)^{20}Ne$.

measured resonant energy, it is not possible to use carbon coating as was done for measurements of iron in gels. To ensure a good evacuation of charges at the surface of the sample, small grids (used in electron microscopy for the same purpose) are put on the polished albite surface. The perfect coincidence of the resonant energies observed for NaCl + C and untreated albite sample is a proof that no static charge appears in the measurements. Other experiments on samples treated for longer time in HCl and NH₄OH solutions are in progress (Demortier et al., 1976).

CONCLUSIONS

Prompt nuclear and atomic reactions induced by protons of energy ranging from a few hundred keV to a few MeV have been applied to elemental analysis of minerals. The method is rapid and at the same time gives all the useful information for quantitative elemental analysis of the great majority of the elements. From this point of view, the technique is very similar to spark source mass spectrometry and ion microprobe analysis, but without the disadvantages of the two last mentioned techniques which are very sensitive to the chemical bond of the elements. Nuclear techniques are therefore more useful for quantitative elemental analysis, with a sensitivity ranging from 1 to 100 ppm for nearly all the elements.

Depth profile analyses of low mass elements are also possible using resonant nuclear reactions. In the particular case of highly diffusible elements (like Na), this non destructive technique is more useful than the ion microprobe (destructive) analyser because resonant nuclear reactions are generated at the beginning of the path of the particle whereas the heating is generated several microns deeper in the material: i.e. at the end of the path of the incident particle (≃ 10 μm). In microprobe analyser these two regions are overlapped.

The technique involving X-ray emission (CPXR) is similar to electron microprobe analysis, but has the disadvantage that the beam size may not be reduced below 5 μm using strong focusing quadrupole magnets (Cookson et al., 1972) or below 20 μm using (L.A.R.N.) three mechanical collimators. The advantages that the CPXR method offers are: (a) the use of well defined linear path of the proton beam compared to the zigzag path of electrons used in electron microprobe analysis, (b) the absence of continuum bremsstrahlung, (c) the less important corrections required to be made for X-ray absorption (Reed, 1975) owing to the fact that proton ranges are very short in minerals and (d) last but not least the attainment of higher sensitivity.

The CPXR method using protons of energy less than 2 MeV has the following advantages over classical X-ray fluorescence (XRF) method: (a) the proton beam has a short range in the sample compared to that of incident X-ray in XRF method and consequently the resulting X-rays that are detected in the

backward direction are less absorbed in the CPXR method; (b) for a given incident proton energy, the production of X-rays is high near the surface of the sample since the cross section for production of X-rays increases with the increase of proton energy and consequently the resulting X-ray absorption may be reduced to a low limit using an appropriate incident proton energy; (c) Although the sensitivity of these two techniques is of the same order of magnitude CPXR method is more rapid (Typical times of bombardment range between 1 and 30 minutes); (d) matrix effects are not important. The amount of material necessary for a panoramic analysis is very low. In most cases, the methods of proton inducing emission of X-ray, γ-ray and α particles, are non destructive.

REFERENCES

Cookson, J. A., Ferguson, A. T. and Pilling, F. D. (1972) Proton microbeams, their production and use: *J. Radioanal. Chem.* **12**, 39–52.

Debras, G. (1975) Analyse de l'azote par réaction (d, α). Rapport L.A.R.N.

Deconninck, G., Demortier, G. and Bodart, F. (1972a) *Proc. Int. meeting Chemical Analysis by Charged Particle Bombardment* Namur, September 1971. Elsevier Sequoia S.A. Lausanne.

Deconnink, G. and Demortier, G. (1972b) Quantitative analysis of Aluminium by prompt nuclear reactions: *J. Radioanal. Chem.* **12**, 189–208.

Deconninck, G. (1972c) Quantitative analysis by (p, γ) and (p, X) reactions at low energies: *J. Radioanal. Chem.* **12**, 157–169.

Deconninck, G. (1973a) Analyse de microquantités d'éléments traces dans des substances solides par bombardment d'ions: *J. Radioanal. Chem.* **17**, 29–43.

Deconninck, G. and Demortier, G. (1973b) Dosage d'échantillons métalliques par réactions nucléaires et atomiques promptes: *Proc. meeting on nuclear Techniques in the Basic Metal Industries*, Helsinki 1972, A.I.E.A. Vienna.

Demortier, G. and Bodart, F. (1972a) Quantitative analysis of phosphorus by (p, γ) reactions: *J. Radioanal. Chem.* **12**, 209–219.

Demortier, G., Gillet, C. and Lefebvre, J. (1972b) Trace element analysis and electrochemical studies of micro-

quantities of biological samples by prompt atomic and nuclear reactions. *Proc. meeting on Nuclear Activation in the Life Sciences*, Bled 1972. A.I.E.A. Vienna.

Demortier, G., Lefebvre, J. and Gillet, C. (1972c) Ion exchange measurement in biological samples by prompt (p, X) and (p, p) reactions: *J. Radioanal. Chem.* **12**, 277–285.

Demortier, G. (1974a) Dosage des éléments légers dans des échantillons biologiques par réactions nucléaires promptes. *Radiochem. Radioanal. Lett.* **16**, 329–341.

Demortier, G. (1974b) La fluorescence-X induite par protons. Applications à l'analyse quantitative: *Le Vide. Les Couches Minces*, suppl. **171**, 224–235.

Demortier, G. (1974c) Prompt analysis of biological samples by proton bombardment: *Radiochem. Radioanal. Lett.* **20**, 197–205.

Demortier, G. and Deconninck, G. (1975a) Thick target excitation yields of prompt γ-rays from proton bombardment of Rh, Pd, Ag, Pt and Au: *J. Radioanal. Chem.* **24**, 437–446.

Demortier, G. and Delsate Ph. (1975b) Analysis of magnesium by prompt nuclear reactions: *Radiochem. Radioanal. Lett.* **21**, 219–224.

Demortier, G., Freund, F. and Jasmund K. (1976) Profile Analysis of Na in Albite Crystals: to be published.

Freund, F., Lindner, B., Demortier, G. and Thone L. (1975a) Cl$^-$ retention by bentonite in the presence of different cations: *Proc. Int. Clay Conf.*, Mexico.

Freund, F. and Lindner, B. (1975b) A soft X-ray spectroscopic study of the interaction between Cl$^-$ and various alkaline cations in aqueous environment: *Proc. Int. Clay Conf.*, Mexico.

Fripiat, J. J. (1973), private communication.

Gordon, B. M. and Kraner, H. W. (1972) On the development of a system for trace element analysis in the environment by charged particle X-ray fluorescence: *J. Radioanal. Chem.* **12**, 181–188.

Ligeon, E. and Bontemps, A. (1972) Nuclear reaction analysis of boron and oxygen in silicon: *J. Radioanal. Chem.* **12**, 329–341.

Liebafsky, H. A., Pfeifer, H. G., Winslow, E. H. and Zemany, P. D. (1960) *X-ray Absorption and Emission in Analytical Chemistry*. Wiley, New York.

Reed, S. J. B. (1975) *Electron Microprobe Analysis*. Cambridge University Press, London.

Tamaki, Y., Omori, T. and Shiowaka, T. (1975) Chemical Effect of the K_α/K_β intensity ratios in the ^{51}Cr-labelled chromium compounds: *Radiochem. Radioanal. Lett.* **20**, 255–262.

Williamson, C. F., Boujot, J-P. and Picard, J. (1966) Tables of range and stopping power of chemical elements for charged particles of energy 0.05–500 MeV: Rapport CEA-R 3042, Paris.